

# Characteristics of interfacial reactions between Ti-6Al-4V alloy and ZrO<sub>2</sub> ceramic mold

Shi-chen Sun<sup>1</sup>, \*Er-tuan Zhao<sup>1</sup>, Chen Hu<sup>1</sup>, Jin-rui Yu<sup>1</sup>, Yu-kun An<sup>1</sup>, Ren-guo Guan<sup>2</sup>

1. School of Mechanical Engineering, Shandong University of Technology, Zibo 255022, China

2. School of Materials Science and Engineering, Dalian JiaoTong University, Dalian 116028, China

**Abstract:** The interfacial reaction between Ti-6Al-4V alloy and ZrO<sub>2</sub> ceramic mold with zirconia sol binder was investigated by keeping the 12 g alloy melt in a vacuum induction furnace for 15 s. The microstructures, element distribution and phase constitution of the interface were identified by optical microscopy (OM), scanning electron microscopy (SEM) equipped with energy dispersive spectroscopy (EDS) and X-ray diffraction (XRD). The results show that the whole interface reaction layer can be divided into three regions: metal penetration layer, transition layer, and hardened layer according to the structure morphology, which has the characteristics of severe metal penetration, finer lamellar, and coarse oxygen-rich  $\alpha$  phase, respectively. The erosion of the alloy melt on the ceramic mold promotes the decomposition of zirconia, which leads to the increase of local Zr concentration, greatly increasing the activity coefficient of Ti, aggravating the occurrence of interfacial reaction. Thus, the interfacial reaction shows the characteristics of chain reaction. When the oxygen released by the dissolution of zirconia exceeds the local solid solubility, it precipitates in the form of bubbles, resulting in blowholes at the interface. The result also indicates that the zirconia mold with zirconia sol binder is not suitable for pouring heavy titanium alloy castings.

**Key words:** titanium alloy; interfacial reaction; ZrO<sub>2</sub> ceramic mold; activity coefficient

**CLC numbers:** TG146.23; **Document code:** A; **Article ID:** 1672-6421(2020)06-409-07



\*Er-tuan Zhao

Male, Ph. D., Associate Professor.  
Research interest: investment casting of titanium alloy. He has published more than 50 papers.

E-mail: etzhao@sdut.edu.cn

Received: 2020-08-04

Accepted: 2020-09-13

Titanium alloys are widely used in aerospace, automotive, marine, biomedical, chemical and other fields owing to their high specific strength, strong corrosion resistance, low elastic modulus, and excellent high temperature and low temperature properties<sup>[1, 2]</sup>. Ti-6Al-4V, which was developed in the early 1950's in the United States<sup>[3]</sup>, is one of the most widely used titanium alloys due to its excellent comprehensive performance. It is reported that about 90% of titanium alloy castings were made of Ti-6Al-4V alloy<sup>[4]</sup>. Ti-6Al-4V alloy has good formability and can be processed by forging, casting, welding, powder metallurgy, etc. Compared with other forming methods, investment casting presents the advantages of higher dimensional precision, lower surface roughness, lower production cost, and higher flexibility in design<sup>[2, 5]</sup>. In particular, investment casting is a very attractive technique to cast complex components of titanium alloys<sup>[5, 6]</sup>. However, it easily reacts with the crucible and ceramic mold during melting and investment casting because of the high reactivity of titanium alloy melt, which deteriorates the surface quality of castings, forms inclusions, and reduces the mechanical properties of titanium castings<sup>[7-9]</sup>.

The interfacial reactions between Ti-6Al-4V alloy and different refractory materials, for instance, BN<sup>[10]</sup>, ZrSiO<sub>4</sub><sup>[11]</sup>, ZrO<sub>2</sub><sup>[12]</sup>, graphite<sup>[13]</sup> and Al<sub>2</sub>O<sub>3</sub><sup>[11, 14]</sup>, have been investigated by many researchers. Our previous studies have confirmed that Y<sub>2</sub>O<sub>3</sub> ceramic mold shows the best stability and the least interface reaction during investment casting, followed by ZrO<sub>2</sub> ceramic mold and then the Al<sub>2</sub>O<sub>3</sub> ceramic mold<sup>[7, 15]</sup>. Many researchers have also confirmed that Y<sub>2</sub>O<sub>3</sub> has good stability as a crucible or ceramic shell<sup>[16-18]</sup>. However, its application is limited due to the high price of Y<sub>2</sub>O<sub>3</sub>. For Al<sub>2</sub>O<sub>3</sub> ceramic mold, the serious interfacial reaction between titanium alloy and Al<sub>2</sub>O<sub>3</sub> leads to the worst mold

filling capacity<sup>[6]</sup>. It seems that  $ZrO_2$  is a suitable material for titanium alloy investment casting. Liu et al.<sup>[19]</sup> investigated the wettability between Ti-6Al-4V melt and  $ZrO_2$  (CaO stabilized) mold, and found that poor wettability can slow down the occurrence of interfacial reaction. Nevertheless, the interfacial reaction time of the above studies is short, which is not consistent with the interfacial reaction of thick titanium alloy castings that takes a long time. Meanwhile, the process and mechanism of a sufficient interfacial reaction remains unclear, which is not conducive to the production of heavy titanium alloy castings.

In the present work, the prolonged interfacial reaction between Ti-6Al-4V alloy and  $ZrO_2$  (CaO stabilized) ceramic mold with zirconia sol binder was carried out to determine whether it is suitable for the production of thick titanium alloy castings using  $ZrO_2$  (CaO stabilized) mold. The process was investigated in detail and the mechanism of interface reaction was revealed.

## 1 Experimental procedure

Ti-6Al-4V button ingot with a mass of 40 g was prepared by a non-consumable electrode vacuum arc melting furnace at first, of which the chemical composition is 5.62wt.% Al, 3.75wt.% V, 0.07wt.% O, and the balance is Ti. The oxygen content in the material was measured by oxygen nitrogen hydrogen analyzer (LECO-TCH600). Then, the melted button ingot was cut into 12 g pieces for the interfacial reaction experiment.

The ceramic mold with a diameter of 20 mm and thickness of 10 mm was fabricated by  $ZrO_2$  (CaO stabilized) powders (325 mesh) and zirconia sol binder according to the traditional investment casting process<sup>[5]</sup>. The dried ceramic mold was baked in an electric furnace at a temperature of 1,000 °C for 2 h.

The zirconia ceramic mold was placed in a U-shaped corundum crucible as the substrate, then the alloy block was placed on it. The specimen was heated to 1,680 °C in an induction melting furnace (V-3, 3-TITAN, Linn High Therm GmbH, Germany) with a vacuum of 0.01 Pa and kept in the melting state for 15 s. After cooling to room temperature in the furnace, the specimen was sectioned longitudinally from the middle, and the sampling position was shown in Fig. 1. The specimen was embedded in epoxy resin, and then ground and mechanical polished, and then sprayed with gold for testing.

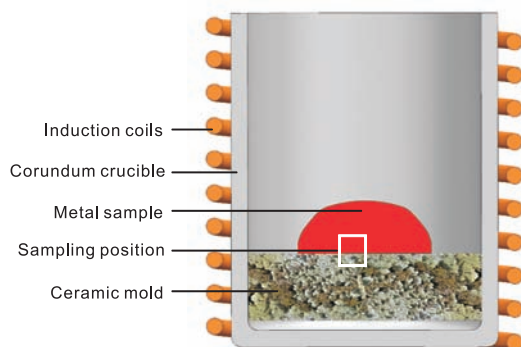


Fig. 1: Schematic diagram of interfacial reaction of specimen

The microstructures and element distribution of the interface were identified by a scanning electron microscope (SEM, FEI Quanta 250) equipped with energy dispersive spectroscopy (EDS). The specimens were etched by Kroll's solution (5%  $HNO_3$ +3%  $HF$ +92%  $H_2O$ , vol.%) to reveal the structure morphology at the interface by optical microscopy (OM, Axio Scope. A1 Zeiss) and SEM.

The phase constitution of interface layer was analyzed by 6000X-ray diffractometer (XRD) with Cu target, and the scanning angle range was from 20° to 100° with an analysis step of 0.02°.

## 2 Results and discussion

### 2.1 Microstructure at interface

Figure 2 shows the metallographic structure of the interface. Although only 15 s was maintained after melting, the characteristics of interfacial reaction were remarkable. The black area on the left is the ceramic mold, and the adjacent dark gray area is the metal penetration layer formed by the metal and ceramic particles, which is a kind of cermet with high hardness and brittleness. There is a thicker  $\alpha$  lamellar area next to the metal penetration layer which is called the hardened layer. According to the research by Sung et al.<sup>[21]</sup>, the  $\alpha$ -case layer formed by the interfacial reaction was composed of the outer reaction layer and the adjacent hardened or diffusion layer. The metal penetration layer and thicker  $\alpha$  lamellar layer in this study can correspond to the reaction layer and hardened layer, respectively. Meanwhile, the blowholes with large diameter can be identified at the interface between the two layers. At the neighboring hardened layer, the matrix structure is typical Widmanstätten structure, and the coarse  $\alpha$  cluster almost runs through the whole grain due to the slow cooling rate.

Figure 3 shows the SEM images of the interface layer. Interestingly, there is a transition layer of about 100  $\mu m$  depth between the metal penetration layer and the hardened layer, which consists of a finer  $\alpha$  lamella. The formation reasons will be discussed in later sections. Therefore, the whole interface reaction layer ( $\alpha$ -case layer in Fig. 2) can be divided into three regions (I, metal penetration layer; II, transition layer; III, hardened layer) according to the structure morphology, as shown in Fig. 3(a). This result is significantly different from that of the research by Sung et al.<sup>[21-23]</sup>. Figure 3(b) is the magnification of partial area I in Fig. 3(a). It can be seen that the alloy melt infiltrated into the shell and fully reacted, resulting in the decomposition of part of the zirconia, from coarse particles to finer particles. It can be seen from Fig. 3(c) that the transition layer is mainly composed of lamellar  $\alpha$  with a average thickness of about 3  $\mu m$  and a small amount of equiaxed  $\alpha$ . Moreover, a large number of small white particles (zirconia) present in the interlamellar region. Figure 3(d) shows the microstructure of the hardened layer. It can be seen that the lamellar  $\alpha$  is relatively thick, which is due to the diffusion of oxygen produced by the interfacial reaction into the alloy matrix, resulting in the formation of coarse  $\alpha$  phase during solidification.

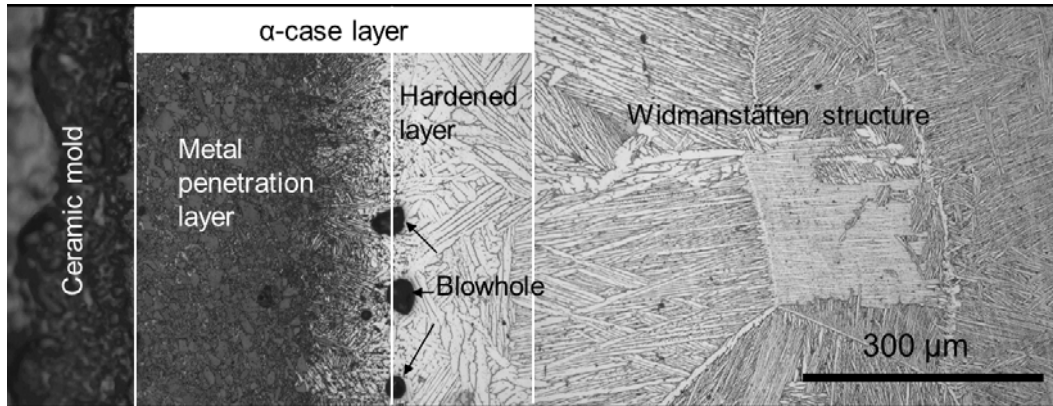


Fig. 2: Metallographic structures of interface between zirconia and Ti-6Al-4V alloy

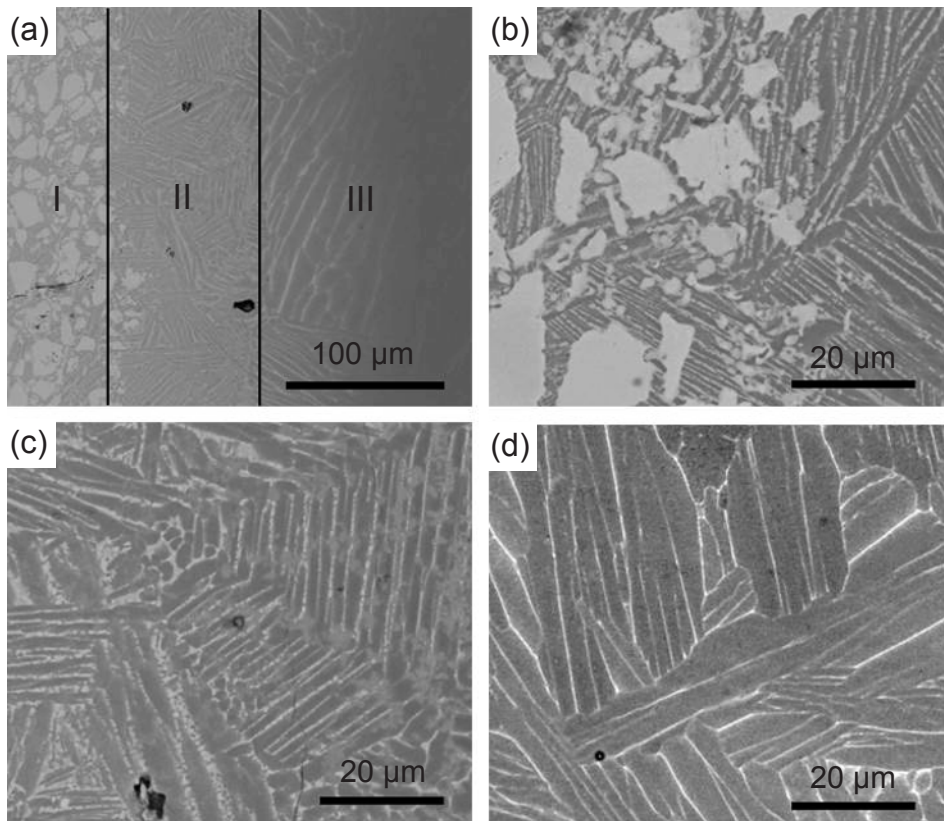


Fig. 3: SEM images of the interface layer between zirconia and Ti-6Al-4V alloy (a), and magnification region I (b), II (c) and III (d) in Fig. 3(a)

## 2.2 Element distribution at interface

The element distribution at the interface characterized by mapping scanning is shown in Fig. 4, which shows that the diffusion of Ti, Zr and O elements is significant, while that of Al and V elements is not so obvious. It can be concluded that the molten titanium alloy infiltrated into the ceramic mold at a deep distance, forming a thick metal penetration layer. In the intermediate transition layer, there are still high concentrations of Zr and O elements, and the diffusion distance of O element is longer, which is related to the smaller atomic radius of interstitial element O and easier diffusion at high temperature. Combined with the results of Fig. 3 and Fig. 4, it is further confirmed that nanometer zirconia exists in the transition layer.

The composition distribution at the interface between

castings and ceramic mold indicates the degree of interfacial reaction and the depth of influence. Figure 5 shows the element line scanning from the metal penetration layer to the matrix alloy. It is obvious that the content of Ti element decreases gradually from the matrix to the interface, while Zr and O elements present the opposite trend. Moreover, the contents of Al and V vary little. The result corresponds with the surface scanning shown in Fig. 4. Therefore, it is deduced that the elements involved in the interfacial reaction are mainly Ti, Zr and O, that is, zirconia decomposes and diffuses into the alloy melt, and the alloy melt spreads to the ceramic shell. From the diffusion distance of the elements, it is demonstrated that the influence depth of the interfacial reaction is much larger than that observed from the microstructure characteristics.



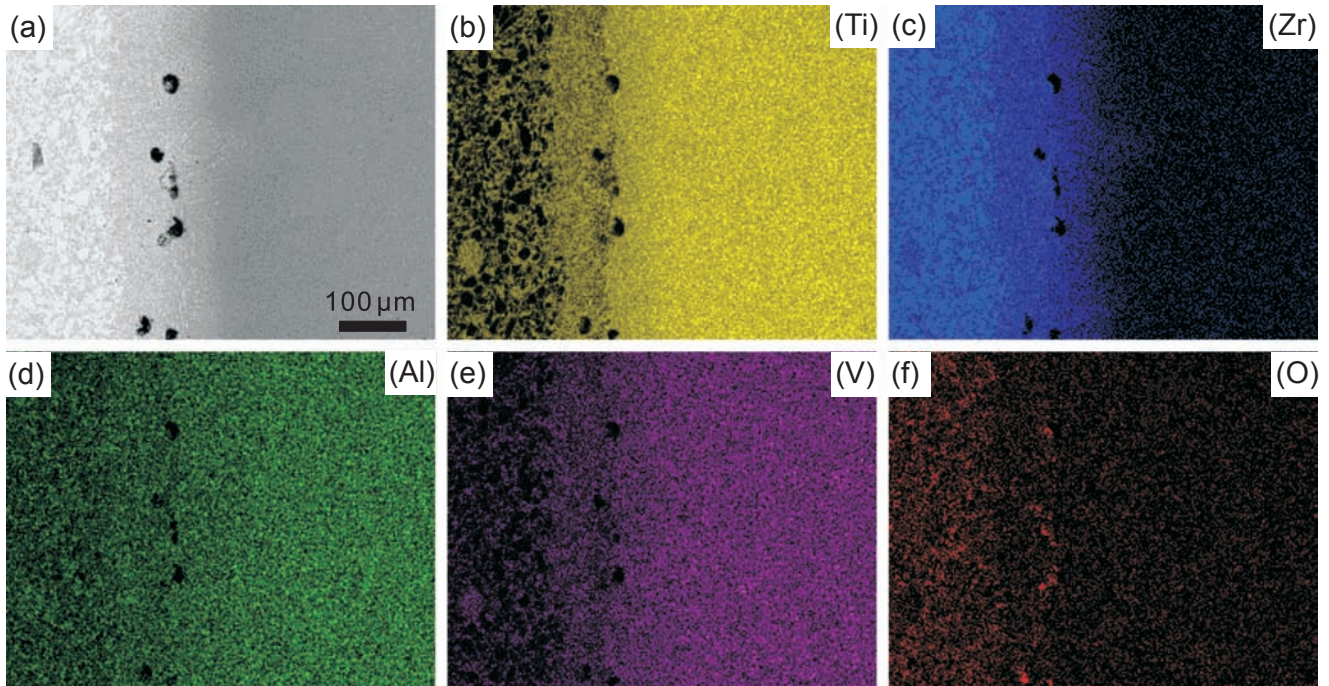


Fig. 4: SEM image (a) and element Ti (b), Zr (c), Al (d), V (e), and O (f) distribution maps of the interface layer

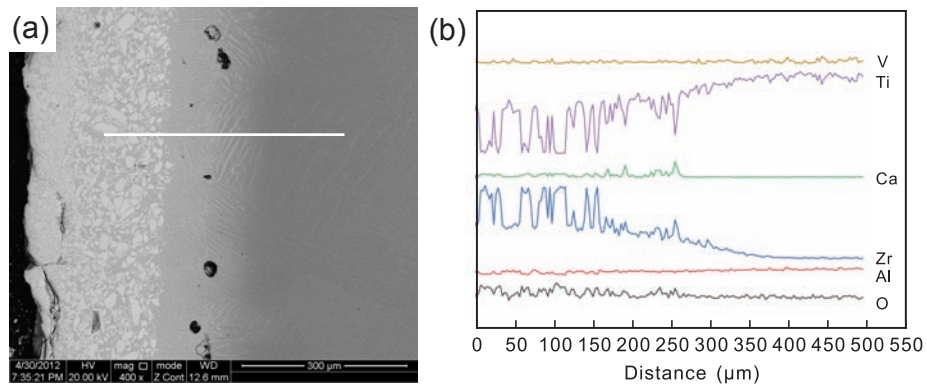


Fig. 5: SEM image (a) and elemental distribution curves (b) of interface layer

### 2.3 Phase constitution at interface

The phase constitution at the interface is shown in Fig. 6. The phase constitution of  $ZrO_2$  powder on the specimen surface that has not been sintered was compared with the phase constitution of the baked zirconia mold, and the result is shown in Fig. 6(a). It can be seen that the baked zirconia mold is mainly composed of stable cubic zirconia with a

small amount of monoclinic zirconia and tetragonal zirconia. The monoclinic zirconia phase near the surface of the casting specimen gradually disappears and the intensity of stable cubic zirconia peak increases, which indicates that the region near the reaction layer is subjected to strong thermal action.

The phase constitution of metal penetration layer is also

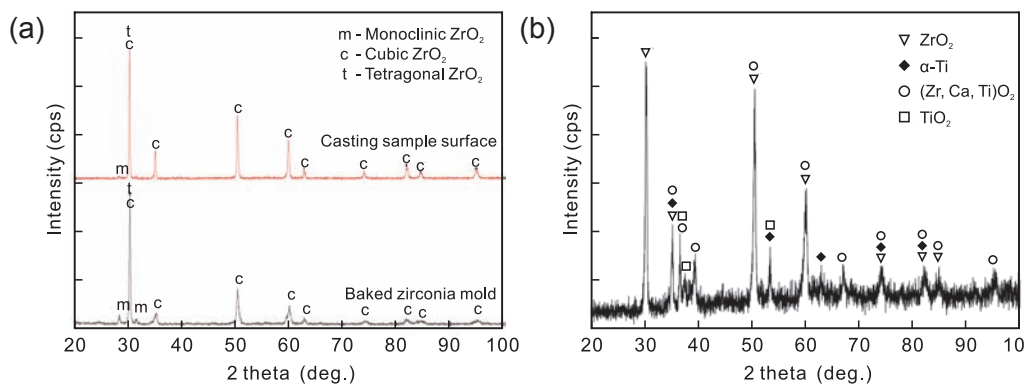


Fig. 6: XRD patterns of powder on specimen surface and baked zirconia mold (a) and metal penetration layer (b)

identified, as shown in Fig. 6(b). The metal penetration layer is still mainly composed of cubic zirconia, and a complex compound  $(\text{Zr, Ca, Ti})\text{O}_2$  and  $\text{TiO}_2$  are also found, which are generated by the reaction between zirconia mold and alloy melt. Due to the infiltration of the alloy melt, the  $\alpha$ -Ti can be seen in the diffraction pattern.

## 2.4 Analysis of interfacial reaction process and mechanism

The Gibbs free energy is often used to analyse the stability of oxide mold and to predict the interfacial reactions. Saha et al. [24] pointed out that the stability of oxides against molten titanium is not completely consistent with Gibbs free energy of forming oxides, and the effect of the dissolution of oxides in liquid metal should be taken into consideration. Cui et al. [25] investigated the dissolution mechanism of oxides and predicted the stability of oxides in molten titanium alloys by thermodynamic analysis, and the calculated results were consistent with the experimental results. Kostov et al. [26] calculated the free energy changes of reaction  $\Delta G_r$  of the different oxides and demonstrated that  $\text{CaO}$ ,  $\text{Y}_2\text{O}_3$ ,  $\text{ZrO}_2$  and  $\text{Al}_2\text{O}_3$  have positive  $\Delta G_r$  values in all compositions of Ti-Al alloys in the temperature range 1,273 K–1,973 K. It seems that these oxides have good stability in terms of thermodynamics and would not dissolve in titanium melt.

In fact, oxide refractories are ion-bonded compounds with high binding energy. However, some atoms may have a low-energy transition and get rid of the inherent energy barrier to become active atoms, due to the defects such as lattice distortion and vacancies in the crystal. If the active atom happens to exist at the reaction interface, it will be absorbed by the surface of the titanium alloy melt and dissolved into the titanium melt. Consequently, the oxide refractories of the surface layer will be gradually eroded by the titanium alloy melt, resulting in interfacial reaction. Lin et al. [23] carried out the thermodynamic calculation of the Gibbs free energy change of the possible reactions between titanium and zirconia, and found that the Gibbs free energies of these reactions are positive or slightly negative, that is to say, these reactions are impossible from the point of view of thermodynamics.

Actually, the interfacial reaction is a complex physical and chemical process, which is affected by many factors. It is well known that the mold is a non-uniform and porous system composed of refractories and binders, as shown in Fig. 7. The zirconia refractory particles are sintered together by the stable zirconia generated by the binder baked at high temperature, forming a continuous three-dimensional structure. This structure has an important influence on the process and characteristics of interfacial reaction between titanium alloy melt and zirconia.

Wei et al. [20] considered that the whole interfacial reaction process can be divided into three stages: surface contact stage, wetting stage and internal reaction stage. However, some researchers pointed out that the interfacial reaction process consists of the decomposition of the ceramic mold and the

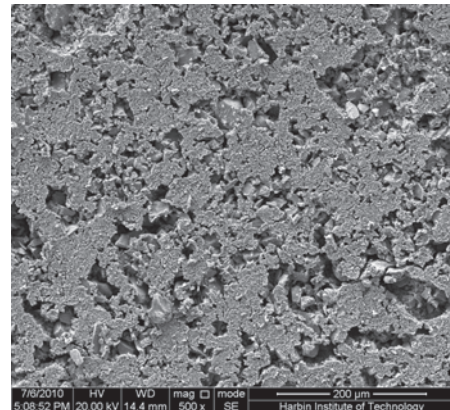
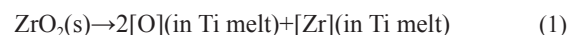


Fig. 7: Surface morphology of  $\text{ZrO}_2$  ceramic mold

diffusion of free elements [21, 27]. Based on the analysis of the microstructure and phase constitution of the interface, the interfacial reaction process and mechanism diagram were established, as shown in Fig. 8. When the alloy melt contacts the ceramic mold surface, it will infiltrate into the gaps between the  $\text{ZrO}_2$  sand grains due to the action of interfacial tension, as shown in Fig. 8(a). In fact, the joint between particles is the most easily eroded by alloy melt. Subsequently, the refractory particles are wrapped in titanium alloy melts. Under the action of thermal erosion, large particles are decomposed into finer particles, and fine particles begin to dissolve, as shown in Fig. 8(b). The reaction can be expressed by the following equation:



The oxygen in the oxide particles is firstly absorbed by the titanium solution and diffused into the alloy melt. When the concentration of local oxygen exceeds its solid solubility, bubbles are easy to precipitate, and these decomposed nano-sized zirconia particles provide the nucleation core for these bubbles. In the process of rising, these small bubbles grow, aggregate, form large bubbles, and finally form pore defects during solidification, which explains why there are large pores in the preface of the transition layer.

The Zr released by the oxide particles is also diffused into the alloy melt and can be dissolved infinitely in titanium alloy. The higher the activity and activity coefficient, the higher the melt activity and the degree of interfacial reaction. Based on Troop's ternary solution model and Miedema's model [28], the activity coefficients of titanium in ternary systems Ti-6Al-xZr and Ti-6Al-xZr ( $x=2, 4, 6, 8, 10$  wt.%) at 2,000 K were calculated. It can be seen from Fig. 9 that the activity coefficient of Ti decreases with the increase of V content, but increases with the increase of Zr content. This result can be attributed to the fact that the Zr and Ti elements belong to the same family, which has the same outer electronic structure and similar atomic radius. It indicates that Zr can form a substitutional solid solution with Ti, and more Ti atoms are replaced with the increase of Zr content, thus increasing the activity coefficient of molten Ti. Thereby, a small "molten pool" is formed in this part, and the alloy melt in the "molten



pool" continues to act on the surrounding zirconia particles under the action of electromagnetic stirring, forming a chain reaction, which leads to a more and more severe interfacial reaction, as shown in the circle in Fig. 8(b). Ultimately, a reaction zone between alloy melt and zirconia refractories is formed.

When the electromagnetic stirring stops, the nano-zirconia particles generated by the decomposition of zirconia in motion begin to float under the action of buoyancy. Due to

the fast solidification rate, the floating zirconia particles are easily captured by the solid-liquid interface, so there are more smaller zirconia particles in the transition layer, which will also play a role in refining the  $\alpha$  lamella. Hence, the  $\alpha$  lamellae in this region are relatively fine. The solidified structure with remarkable fine grain characteristics was formed, as shown in Fig. 8(c).

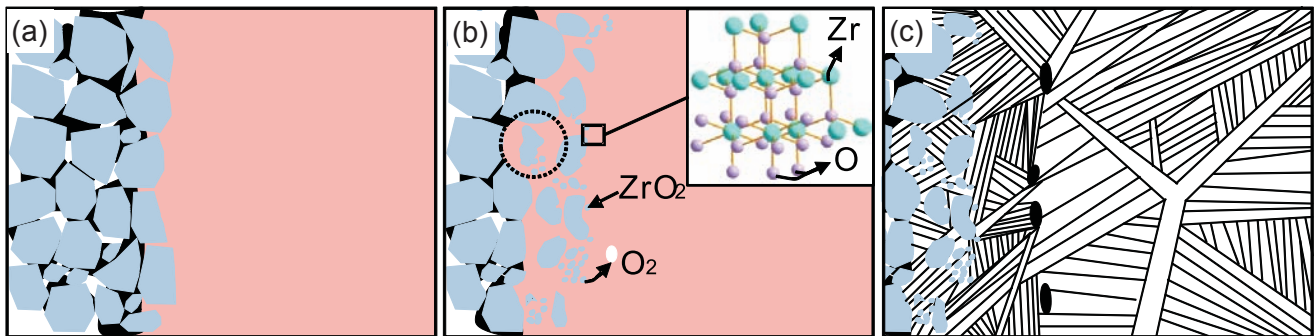


Fig. 8: Schematic illustration of interaction between Ti-6Al-4V melt and  $ZrO_2$  ceramic mold: (a) erosion; (b) chain reaction; (c) solidification

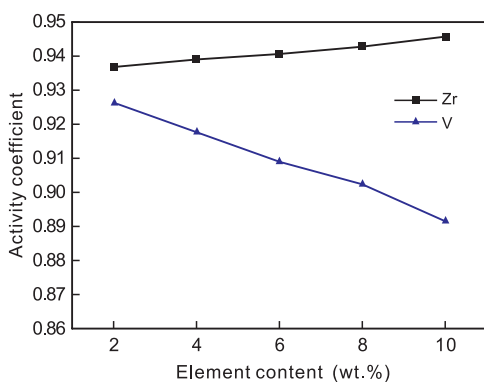


Fig. 9: Effect of element content on the activity coefficient of Ti

### 3 Conclusions

(1) The interface reaction between Ti-6Al-4V and zirconia shell is severe, and the reaction layer is composed of: metal penetration layer, transition layer and hardened layer. Large pores appear between the transition layer and the hardened layer.

(2) The interfacial reaction begins with the infiltration of the alloy melt into the mold surface, which causes the decomposition of the baked binder products, resulting in the shedding of refractory particles. The particles are wrapped in the alloy melt and further decomposed. The activity coefficient of Ti in the local alloy melt increases due to the release of Zr atom from the dissolution of zirconia, which aggravates the reaction and makes the interface reaction show the characteristic of continuity.

(3) The experimental results show that the zirconia mold with zirconia sol binder is not suitable for pouring heavy titanium alloy castings, and the binder with more stable thermodynamics should be selected, or the pouring temperature and shell preheating temperature should be reduced properly to slow down the interfacial reaction.

### Acknowledgments

This work was supported financially by the National Natural Science Foundation of China (Grant No. 51871184) and the Natural Science Foundation of Shandong Province (Grant No. ZR2017MEE038), and China Postdoctoral Science Foundation (No. 2018M642683).

### References

- [1] Peters M, Kumpfert J, Ward C H, et al. Titanium alloys for aerospace applications. *Advanced Engineering Materials*, 2003, 5(6): 419–427.
- [2] Cui C X, Hu B M, Zhao L C, et al. Titanium alloy production technology, market prospects and industry development. *Materials & Design*, 2011, 32(3): 1684–1691.
- [3] Leyens C, Peters M. Titanium and titanium alloys: Fundamentals and applications. Wiley-VCH: Cologne, 2003.
- [4] Nastac L, Gungor M N, Uco I, et al. Advances in investment casting of Ti-6Al-4V alloy: A review. *International Journal of Cast Metals Research*, 2006, 19(2): 73–93.
- [5] Pattnaik S, Karunakar D B, Jha P K. Developments in investment casting process—A review. *Journal of Materials Processing Technology*, 2012, 212(11): 2332–2348.
- [6] Chen Y Y, Zhao E T, Kong F, T et al. Fabrication of thin-walled high-temperature titanium alloy component by investment casting. *Materials and Manufacturing Processes*, 2013, 28(6): 605–609.
- [7] Zhao E T, Kong F T, Chen Y Y. Effect of different primary coating materials and mold temperatures on fluidity of high-temperature titanium alloy. *Proceedings of the Institution of Mechanical Engineers, Part B: Journal of Engineering Manufacture*, 2012, 226(11): 1862–1868.
- [8] Liu A H, Li B S, Sui Y W, et al. Research progress of interfacial reaction between titanium alloys and molds. *Rare Metal Materials and Engineering*, 2012, 41(3): 554–558.
- [9] Cen M J, Liu Y, Chen X, et al. Inclusions in melting process of titanium and titanium alloys. *China Foundry*, 2019, 16(4): 223–231.

- [10] Liu H B, Shen B, Zhu M, et al. Reaction between Ti and boron nitride based investment shell molds used for casting titanium alloys. *Rare Metals*, 2008, 27(6): 617–622.
- [11] Chamorro X, Herrero-Dorca N, Rodriguez P P, et al. Alpha-case formation in Ti-6Al-4V investment casting using ZrSiO<sub>4</sub> and Al<sub>2</sub>O<sub>3</sub> moulds. *Journal of Materials Processing Technology*, 2017, 243: 75–81.
- [12] Lin K F, Lin C C. Interfacial reactions between zirconia and titanium. *Scripta Materialia*, 1998, 39(10): 1333–1338.
- [13] Wang L, Yan H, Teng J, et al. Effect of hydrogen on interfacial reaction between Ti-6Al-4V alloy melt and graphite mold. *Journal of Materials Research and Technology*, 2020, 9(3): 6933–6939.
- [14] Wang L, Liu X D, Wang M, et al. Effects of hydrogen on the interfacial reaction between Ti6Al4V alloy melt and Al<sub>2</sub>O<sub>3</sub> ceramic shell. *International Journal of Hydrogen Energy*, 2018, 43(10): 5225–5230.
- [15] Zhao E T, Kong F T, Chen Y Y, et al. Interfacial reactions between Ti-1100 alloy and ceramic mould during investment casting. *Transactions of Nonferrous Metals Society of China*, 2011, 21: s348–s352.
- [16] Lu M W, Lin K L, Lin C C. Interfacial reactions between Ti and Y<sub>2</sub>O<sub>3</sub>/Ca<sub>4</sub>Ti<sub>3</sub>O<sub>10</sub> composites. *International Journal of Applied Ceramic Technology*, 2020, 17(3): 864–873.
- [17] Cui R J, Tang X X, Gao M, et al. Microstructure and composition of cast Ti-47Al-2Cr-2Nb alloys produced by yttria crucibles. *Materials Science and Engineering A: Structural Materials Properties Microstructure and Processing*, 2012, 541: 14–21.
- [18] Gao M, Jia L N, Tang X X, et al. Interaction mechanism between niobium-silicide-based alloy melt and Y<sub>2</sub>O<sub>3</sub> refractory crucible in vacuum induction melting process. *China Foundry*, 2011, 8(2): 190–196.
- [19] Liu A H, Li B S, Yan D G, et al. Wettability of Ti6Al4V on calcia-stabilized zirconia. *Materials Letters*, 2012, 73: 40–42.
- [20] Wei Y M, Hu K H, Lu Z G. Effect of SiO<sub>2</sub> concentration in silica sol on interface reaction during titanium alloy investment casting. *China Foundry*, 2018, 15(1): 23–30.
- [21] Sung S Y, Kim Y J. Alpha-case formation mechanism on titanium investment castings. *Materials Science and Engineering: A*, 2005, 405 (1–2): 173–177.
- [22] Sung S Y, Choi B J, Han B S, et al. Evaluation of alpha-case in titanium castings. *Journal of Materials Science & Technology*, 2008, 24(1): 70–74.
- [23] Lin K F, Lin C C. Interfacial reactions between Ti-6Al-4V alloy and zirconia mold during casting. *Journal of Materials Science*, 1999, 34(23): 5899–5906.
- [24] Saha R L, Nandy T K, Misra R D K, et al. On the evaluation of stability of rare-earth-oxides as face coats for investment-casting of titanium. *Metallurgical and Materials Transactions B: Process Metallurgy and Materials Processing Science*, 1990, 21(3): 559–566.
- [25] Cui R J, Tang X X, Gao M, et al. Thermodynamic analysis of interactions between Ti-Al alloys and oxide ceramics. *Transactions of Nonferrous Metals Society of China*, 2012, 22(4): 887–894.
- [26] Kostov A, Friedrich B. Predicting thermodynamic stability of crucible oxides in molten titanium and titanium alloys. *Computational Materials Science*, 2006, 38(2): 374–385.
- [27] Oliveira P C G, Adabo G L, Ribeiro R F, et al. The effect of mold temperature on castability of CP Ti and Ti-6Al-4V castings into phosphate bonded investment materials. *Dental Materials*, 2006, 22(12): 1098–1102.
- [28] Ding X Y, Fan P, Wang W Z. Thermodynamic calculation for alloy systems. *Metallurgical and Materials Transactions B: Process Metallurgy and Materials Processing Science*, 1999, 30(2): 271–277.